Supplementary information

Mutations in *ISPD* cause Walker-Warburg syndrome and defective glycosylation of α-dystroglycan

Tony Roscioli[1], Erik-Jan Kamsteeg[1], Karen Buysse[1], Isabelle Maystadt[1], Jeroen van Reeuwijk, Christa van den Elzen, Ellen van Beusekom, Moniek Riemersma, Rolph Pfundt, Lisenka E.L.M. Vissers, Margit Schraders, Umut Altunoglu, Michael F. Buckley, Han G. Brunner, Bernard Grisart, Huiqing Zhou, Joris A. Veltman, Christian Gilissen, Grazia M.S. Mancini, Paul Delrée, Michèl A. Willemsen, Danijela Petković Ramadža, David Chitayat, Christopher Bennett, Eamonn Sheridan, Els A.J. Peeters, Gita M.B. Tan-Sindhunata, Christine E. de Die-Smulders, Koenraad Devriendt, Hülya Kayserili, Osama Abd El-Fattah El-Hashash, Derek L. Stemple, Dirk J. Lefeber, Yung-Yao Lin[2], Hans van Bokhoven[2]

[1]These authors contributed equally to this work; [2]These authors jointly directed this work.

Correspondence: Yung-Yao Lin, PhD, Wellcome Trust Sanger Institute, Wellcome Trust Genome Campus, Hinxton, Cambridge, CB10 1SA, United Kingdom, and Hans van Bokhoven, PhD, Department of Human Genetics 855, Radboud University Nijmegen Medical Centre, Nijmegen, P.O. Box 9101, 6500 HB Nijmegen, The Netherlands. Email: YYL@sanger.ac.uk & H.vanbokhoven@gen.umcn.nl

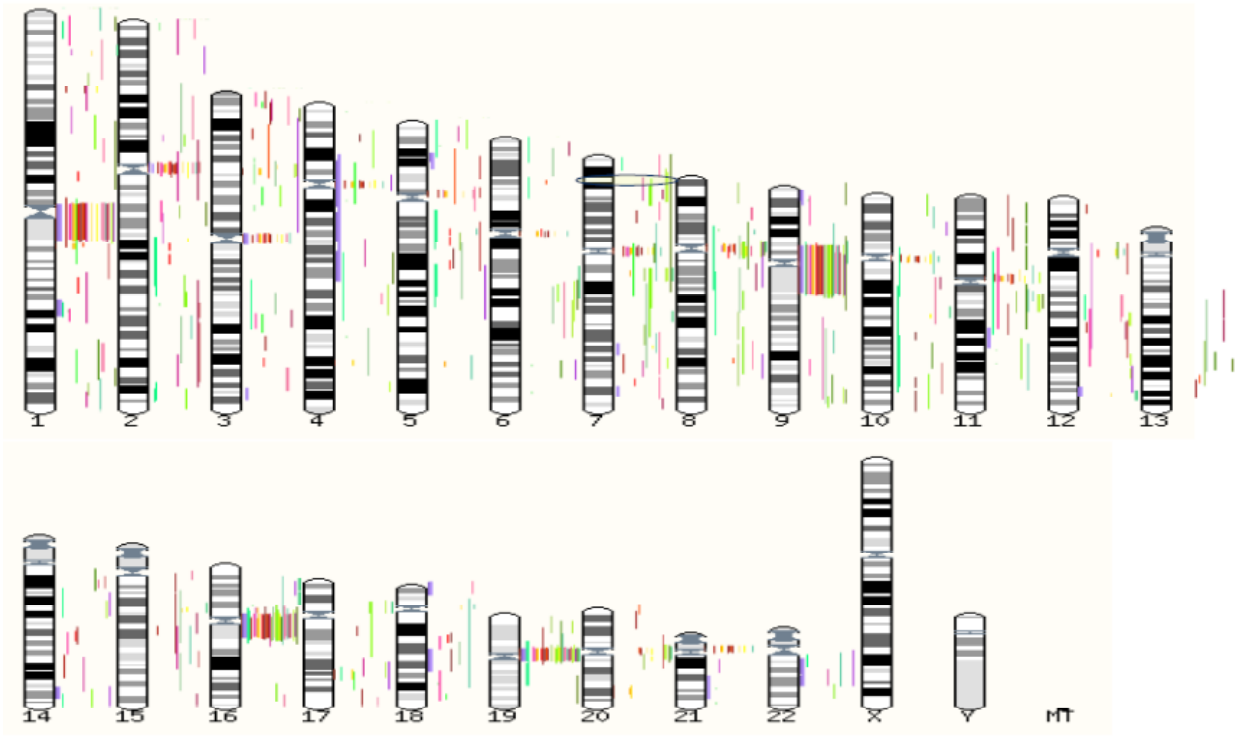

Supplementary Figure 1: Homozygosity mapping results for 30 unsolved patients (prescreened for the known dystroglycanopathy genes). Ideograms showing the 20 largest homozygous regions for each WWS patient. Affected siblings are coded with the same color, and different colors are used for separate families. The *ISPD* region on chromosome 7p21 is circled showing that it is not visibly different to other regions of overlap. Multiple regions of overlap suggest that more WWS genes are yet to be identified.

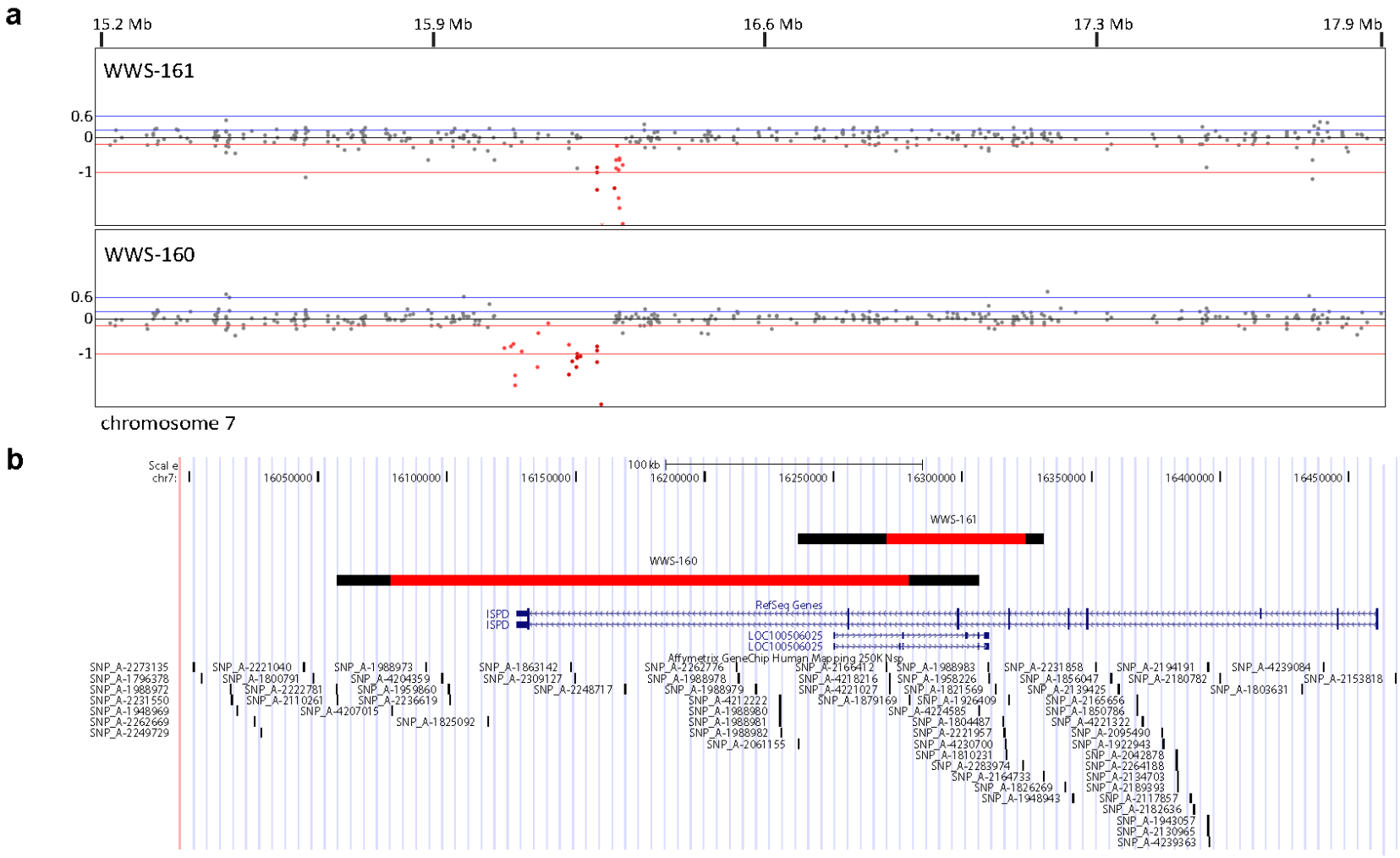

Supplementary Figure 2

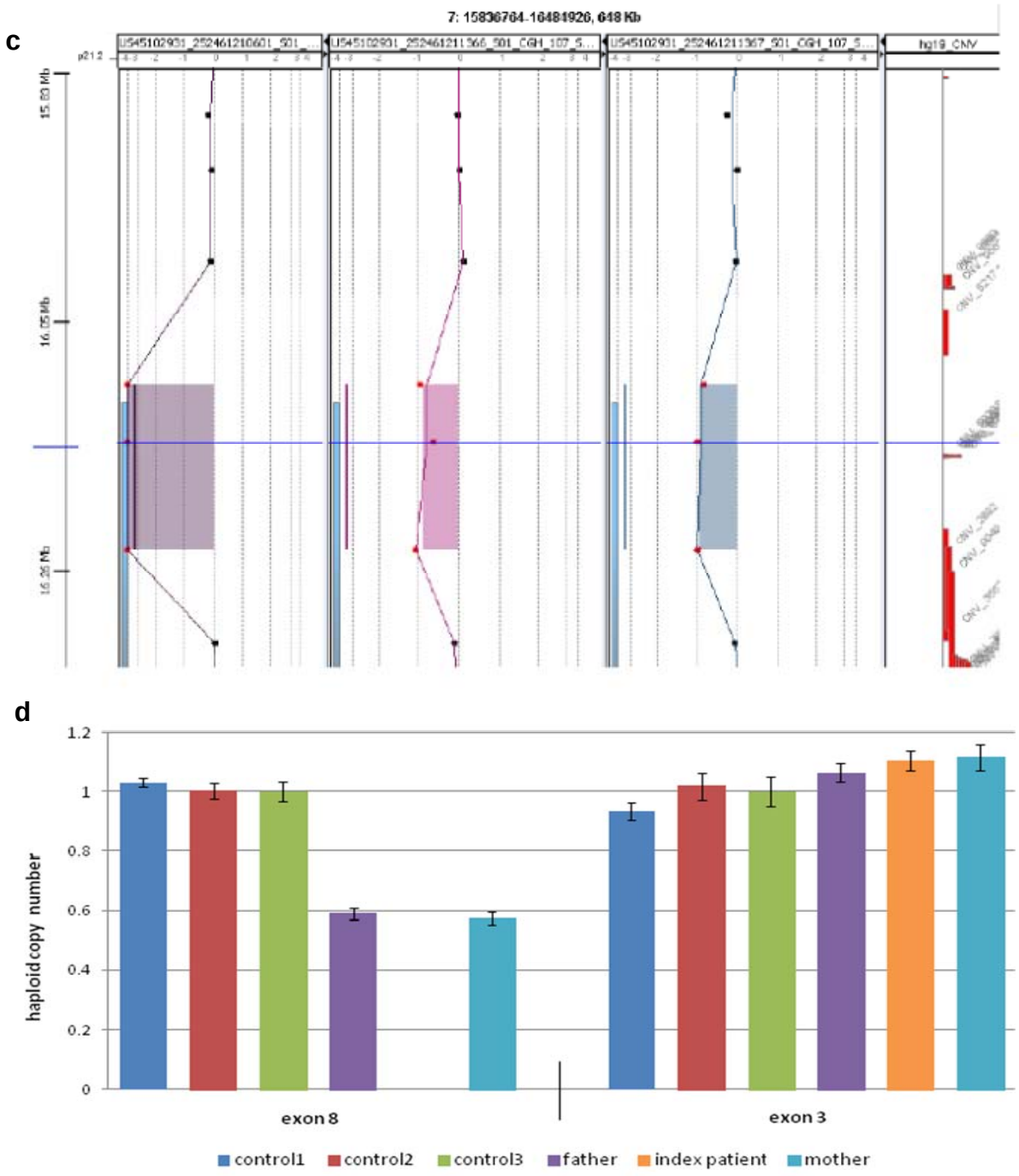

Supplementary Figure 2 (continued): ArrayCGH results for patient WWS-160 and WWS-161. (a) Log_2-ratio profile from the Affymetrix GeneChip Human Mapping 250K array for part of chromosome 7 (15.2 to 17.9 Mb). Deleted probes (15 and 21 for WWS-161 and 160 respectively) are indicated in red. (b) UCSC genome browser view of the homozygous deletions. The position of the SNPs from the probes on the array is indicated. The minimum deleted region is shown in red, the maximum deleted region in black. (c) ArrayCGH profile from the Agilent

Genomic Workbench (60K oligonucleotide array) showing part of chromosome 7 (15.83 to 16.48 Mb). From left to right: patient, mother and father of family WWS-160. The *ISPD* deletion is present in the homozygous state in the patient and in the heterozygous state (log_2=-1) in both parents. (d) Genomic qPCR analysis of exon 8 (deleted) and exon 3 (not deleted) in family WWS-161, confirming the homozygous deletion in the patient and showing heterozygosity in both parents.

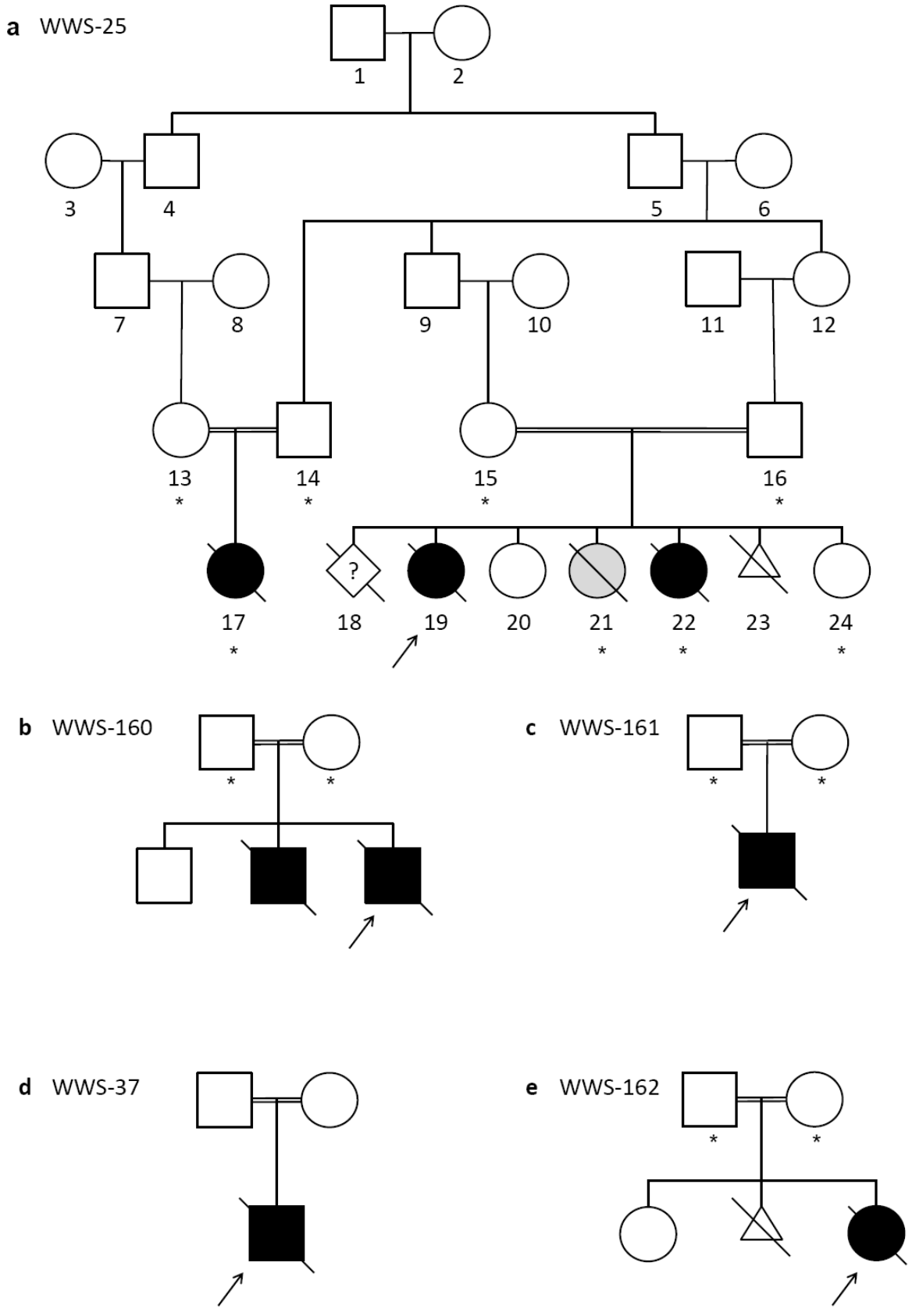

Supplementary Figure 3

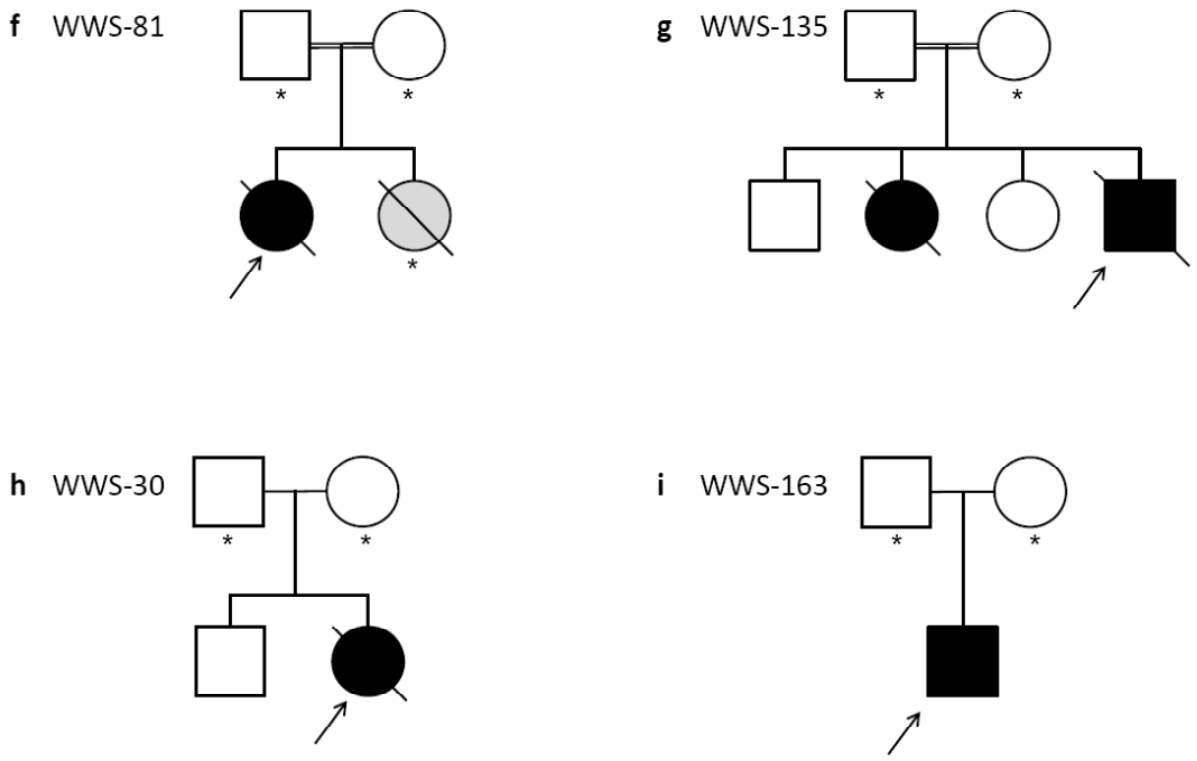

Supplementary Figure 3 (continued): Pedigrees for the 9 families in which *ISPD* mutations were detected. Black symbols indicate individuals affected with WWS. Grey symbols indicate individuals affected with a disease other than WWS. In each family, the proband is indicated by an arrow. Asterisks (*) indicate the availability of DNA samples for segregation studies.

a

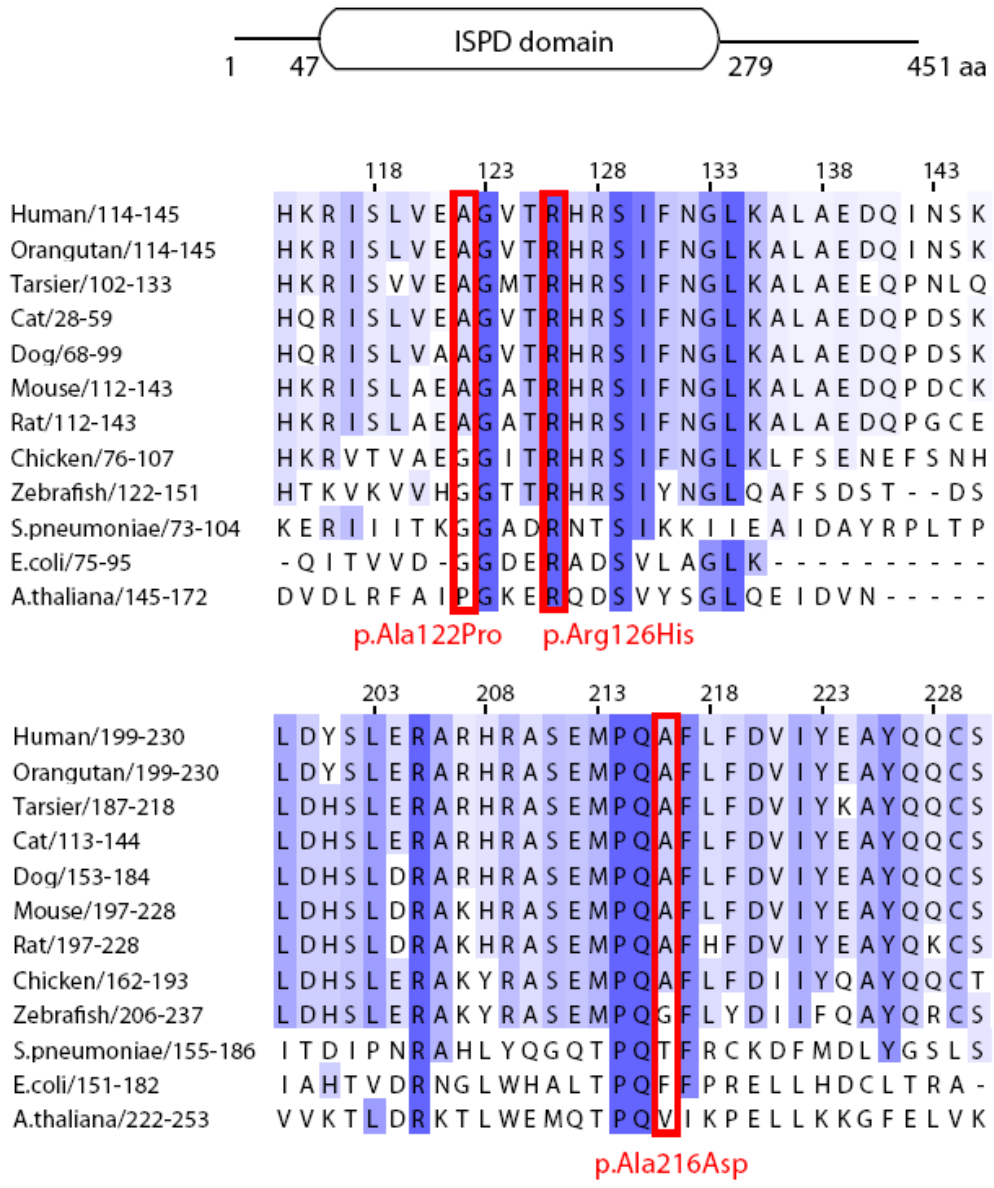

Supplementary Figure 4

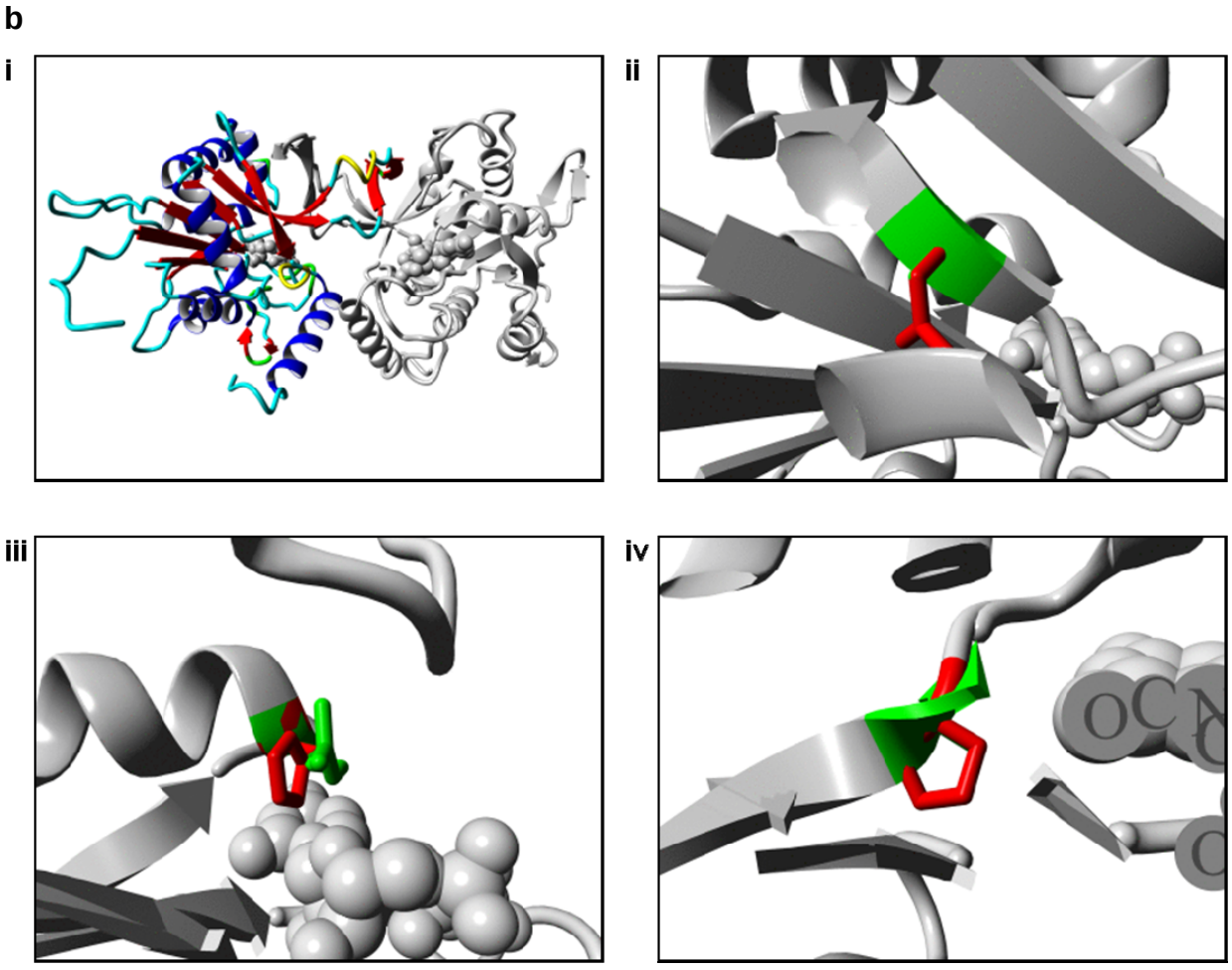

Supplementary Figure 4 (continued): Evaluation of missense mutations. (a) Multiple sequence alignment of ISPD. Human ISPD is shown schematically on top. Darker shades of blue indicate higher levels of conservation. The missense mutations p.Ala122Pro, p.Arg126His and p.Ala216Asp are indicated by solid red boxes. (b) ISPD in ribbon representation showing (i) ISPD dimer with detail of ligand binding site and a potential ligand, CTP (cytidine triphosphate) as a ball model. Color code is blue for α-helix, red for β-strand, green for turn, yellow for 3/10 helix and cyan for random coil. Close-up of mutated amino acids including (ii) p.Ala216Asp, (iii) p.Ala122Pro and (iv) p.Arg126His. The protein is colored grey, the side-chains of the wild type and mutated residue are represented in green and red respectively, showing bulky side-chain and loss of hydrophobicity (p.Ala216Asp) and interruption of binding to CTP (p.Arg126His and p.Ala122Pro).

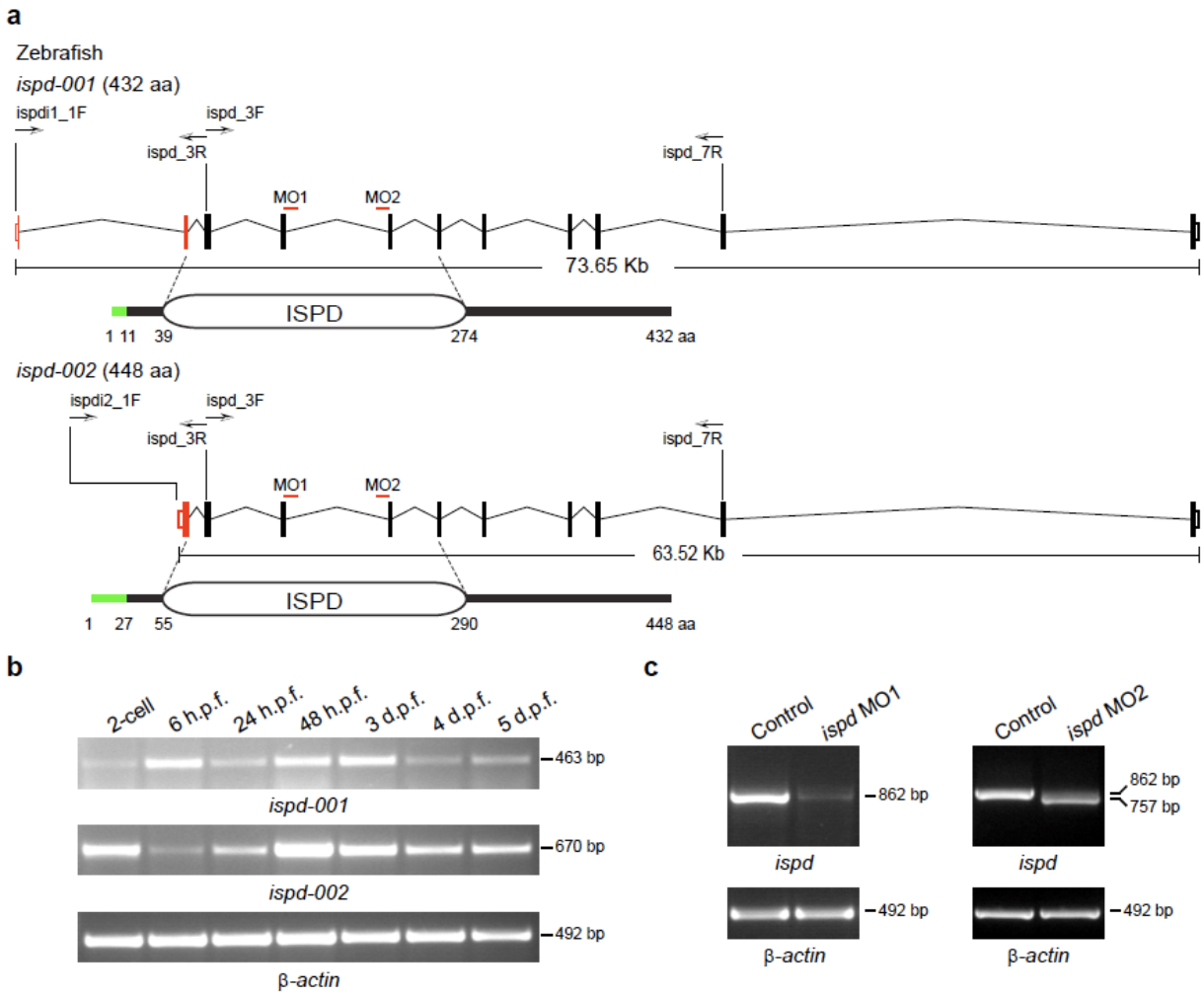

Supplementary Figure 5: Alternative spliced zebrafish *ispd* transcripts, temporal gene expression and MO specificity. (a) Schematic representation of zebrafish *ispd* gene structure and two isoforms. Unique exons of the zebrafish *ispd* transcripts are indicated in red, whereas the common exons are in black. Open rectangles represent untranslated regions. *ispd* MO1 and MO2 target against exon-intron splice sites common to both transcripts. The two Ispd isoforms differ only in their N-termini (green) before the highly conserved ISPD domain (oval box). Common amino acids are indicated in black. Arrows represent the positions of primers used (See **Supplementary Table 2** for primer sequences). (b) Both *ispd* transcripts could be detected by reverse transcriptase-PCR (RT-PCR) during the first 5 days of zebrafish development. *ispd-001* and *ispd-002* were detected using primer ispd_3R with primer ispdi1_1F and ispdi2_1F, respectively. h.p.f. (hours post fertilization); d.p.f. (days post fertilization). *In situ* hybridization by Thisse *et al.*[1] showed ubiquitous expression of zebrafish *ispd* from 1-cell stage to 60 h.p.f. (c) Compared with controls, RT-PCR of embryos injected with *ispd* MO1 (7 ng) showed nearly

absence of PCR product (862 bp), indicating a lack of functional transcripts. Similarly, the normal-length transcripts were almost absent in embryos injected with *ispd* MO2 (3 ng), and instead a smaller PCR product (757 bp) was detected. Sequencing of this product revealed the skipping of the entire target exon (105 bp), resulting in an in-frame deletion within the highly conserved ISPD domain, which may affect the normal function of the protein. Primers ispd_3F and ispd_7R were used in both RT-PCR experiments.

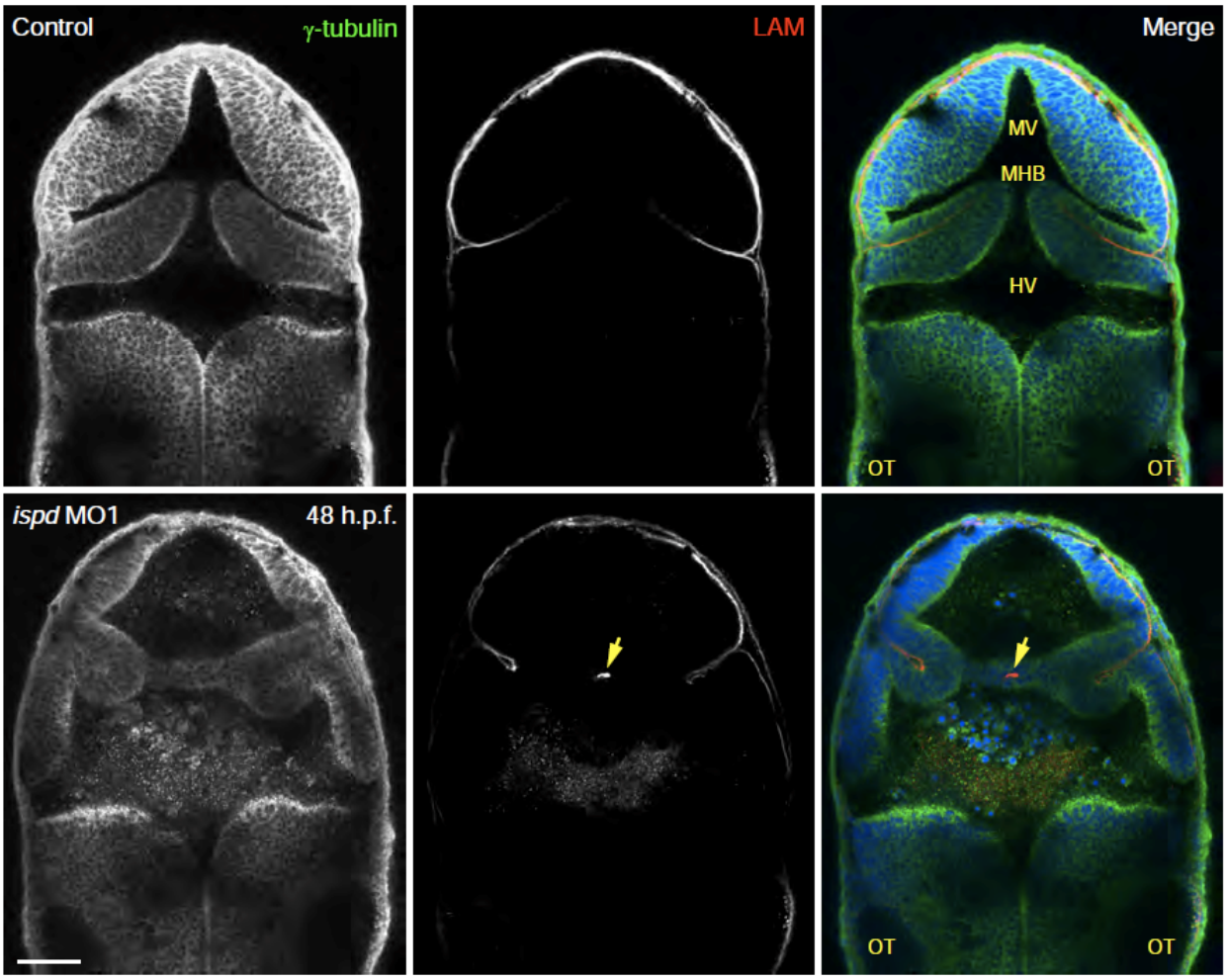

Supplementary Figure 6: Abnormal brain morphology associated with ectopic laminin deposition in *ispd* MO1-injected zebrafish embryos. Neuroepithelial cells are labeled with γ-tubulin (green) and the basement membrane is indicated by laminin immunoreactivity (red). Nuclei are labeled by DAPI (blue). Note that ectopic laminin deposition (arrow) is seen between two midbrain-hindbrain boundary (MHB) folds in *ispd* MO1-injected embryos. MV, midbrain ventricle. HV, hindbrain ventricle. OT, otic vesicle. Scale bar, 50 μm.

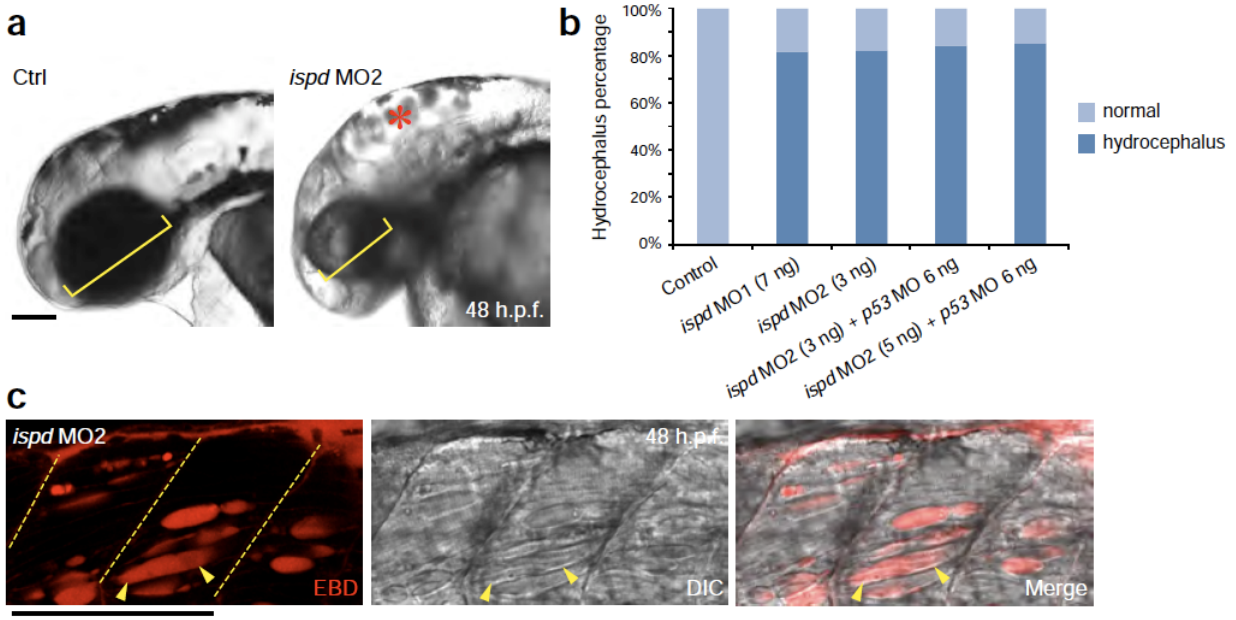

Supplementary Figure 7: Injection of *ispd* MO2 caused eye, brain and muscle defects similar to those in *ispd* MO1-injected embryos. (a) Compared with controls, embryos injected with *ispd* MO2 (3 ng) displayed hydrocephalus (asterisk) and reduced eye size (brackets) at 48 h.p.f. (b) Injection of either *ispd* MO1 (7 ng) or *ispd* MO2 (3 ng) caused hydrocephalus in 82% of embryos at 48 h.p.f. (n=88 and 90, respectively). Co-injection of *p53* MO (6 ng) with *ispd* MO2 (3 ng or 5 ng) still caused hydrocephalus (84%, n=89 and 85%, n=82, respectively), suggesting that this phenotype was not due to MO off-target effects mediated by p53-induced cell death. (c) Similar to *ispd* MO1-injected embryos, embryos injected with *ispd* MO2 (3 ng) revealed that muscle fibers anchored at MTJ (arrowheads) were infiltrated by EBD at 48 h.p.f., suggesting compromised sarcolemma integrity before the onset of muscular dystrophy. Dashed lines represent MTJ. Scale bar, 100 μm.

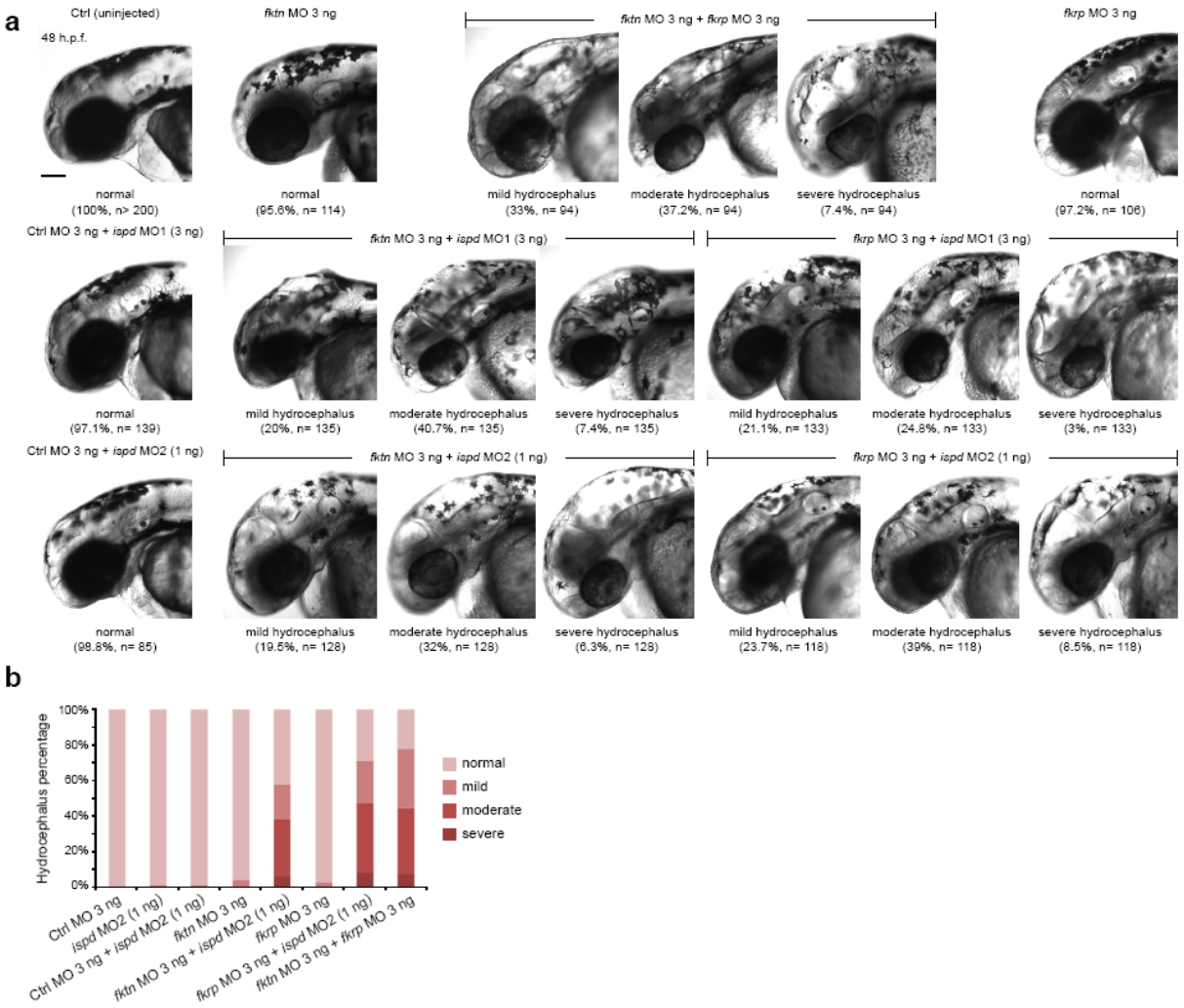

Supplementary Figure 8: Genetic interactions between *ispd*, *fktn* and *fkrp*. (a) Sub-effective doses of *ispd* MO1 (3 ng), *ispd* MO2 (1 ng), *fktn* MO (3 ng) and *fkrp* MO (3 ng) were injected together or alone. Compared with co-injection of control MO (3 ng) and *ispd* MO1 (3 ng), *ispd* MO1 co-injected with either *fktn* MO or *fkrp* MO caused a marked increase of percentage of embryos with mild, moderate and severe hydrocephalus. Similar synergistic effects could be observed using sub-effective doses of *ispd* MO2 instead of *ispd* MO1. In addition, co-injection of *fktn* and *fkrp* MOs also caused a marked increase of hydrocephalus. These results suggest that *ispd*, *fktn* and *fkrp* genetically interact with one another. Scale bar, 100 µm. (b) A chart shows that *ispd* MO2 exerts the same synergistic effect with *fktn* or *fkrp* MOs, as compared with *ispd* MO1 (see also **Fig. 4d**). Each bar represents a combination of two independent experiments scored blindly, n=83–128 embryos.

Supplementary Table 1: Clinical features of the *ISPD* mutation positive WWS/MEB cohort

Patient	**WWS-25.19**	**WWS-25.22**	**WWS-25.17**	**WWS-160**	**WWS-161**	**WWS-37**
Cortical abnormalities	Cobblestone lissencephaly	Cobblestone lissencephaly	Cobblestone lissencephaly	Not clear (severe hydrocephalus)	Cobblestone lissencephaly	Cobblestone lissencephaly
Hydrocephalus	Yes	Yes	Yes	Yes	Yes	Yes
Corpus callosum	Hypoplasia	NA	NA	Hypoplasia	Partial agenesis	Hypoplasia
Encephalocele	Yes	No	No	No	Yes	No
Cerebellar abnormalities	Yes	Yes	Yes	No	Yes	Yes
Brainstem kinking	Yes	NA	Yes	NA	Yes	Yes
Microphthalmia/ retinal abnormalities	Right/-	No	NA	Left/ thin retina	Yes/-	Left/ bilateral retinal detachment, choroidal abnormalities
Congenital cataract	Bilateral cloudy cornea	Bilateral	Right	No	Yes	Left
Anterior chamber abnormalities	Left shallow	Buphthalmos, Peter's anomaly	PHPV left	Glaucoma, corneal oedema	PHPV	Bilateral glaucoma
Serum CK (NR<200 U/l)	104,769	6,543	>2,000	41,206	NA	5,725
Muscular dystrophy/ hypotonia	Yes	Yes	Yes	Yes	NA	Yes
Alpha DG staining	Reduced	NA	NA	Reduced	NA	NA
Age of death	Neonatal period	13 months	9 months	9 days	4 months	14 months

CK, creatine kinase; DG, dystroglycan; NA, not available; PHPV, persistent hyperplastic primary vitreous

Supplementary Table 1 (continued): Clinical features of the *ISPD* mutation positive WWS/MEB cohort

Patient	WWS-162	WWS-81	WWS-135	WWS-30	WWS-163
Cortical abnormalities	Cobblestone lissencephaly	Cobblestone lissencephaly	Cobblestone lissencephaly	Cobblestone lissencephaly	Pachygyria and polymicrogyria
Hydrocephalus	Yes	Yes	Yes	Yes	No
Corpus callosum	Agenesis	NA	Hypoplasia	Hypoplasia	Hypoplasia
Encephalocele	No	No	No	No	No
Cerebellar abnormalities	Yes	Yes	Yes	Yes	Yes
Brainstem kinking	Yes	NA	Yes	Yes	No
Microphthalmia/ retinal abnormalities	NA	-/retinal detachment	Bilateral/hyper-plastic vitreous, optic atrophy	-/retinal dysgenesis	Right/retinal detachment and optic atrophy
Congenital cataract	NA	Bilateral	Bilateral		No
Anterior chamber abnormalities	NA	Synechiae	shallow	NA	Glaucoma
Serum CK (NR<200 U/l)	NA	1,929	2,790	2,500	9,366
Muscular dystrophy/ hypotonia	NA	Yes	Yes	Yes	Yes
Alpha DG staining	NA	Reduced	NA	NA	NA
Age of death	23+5 weeks of gestational age	2.5 years	2 years	2 years	still alive (5.5 years)

CK, creatine kinase; DG, dystroglycan; NA, not available

Supplementary Table 2: Primer and morpholino sequences, product sizes and annealing temperatures (T_a) for amplification of human (Hs) *ISPD* exons from genomic DNA and zebrafish (Dr) *ispd* and *bactin* products from cDNA.

primer/ morpholino	sequence (5' to 3')	size (bp)	T_a (°C)	species
ISPD_1_F	tgtaaaacgacggccagtGTGGTCTGCCCTTCGCC			
ISPD_1_R	caggaaacagctatgaccTAGCGCTAGAGCAGCGG	434	60	Hs
ISPD_2_F	tgtaaaacgacggccagtACCAATACTAGTGATTCAATTTTCTG			
ISPD_2_R	caggaaacagctatgaccTCACCATAACATCTTTAGGTCATC	496	60	Hs
ISPD_3_F	tgtaaaacgacggccagtCAGAATTTCACTTTAAAATGGCTTG			
ISPD_3_R	caggaaacagctatgaccAAATGTGGAGGTTGTTTGGG	276	60	Hs
ISPD_4_F	tgtaaaacgacggccagtCCCTTCCTTTGTTTGCAATG			
ISPD_4_R	caggaaacagctatgaccTCAATGCACTACTGGTTTTAAATG	288	60	Hs
ISPD_5_F	tgtaaaacgacggccagtATTGCTTGCACATTCCTTCC			
ISPD_5_R	caggaaacagctatgaccTGAGAAATTCCGAACTGGC	170	60	Hs
ISPD_6_F	tgtaaaacgacggccagtTGGCCTGAAATCAAAACCTC			
ISPD_6_R	caggaaacagctatgaccCTGGCAGACCAAAGGATCTC	375	60	Hs
ISPD_7_F	tgtaaaacgacggccagtATGGTCCTTGGCTTTATGGG			
ISPD_7_R	caggaaacagctatgaccTTGTCCAAAATACCACTCTTCTC	396	60	Hs
ISPD_8_F	tgtaaaacgacggccagtTGCAGAATCTCTCCATTTATTCC			
ISPD_8_R	caggaaacagctatgaccTTGAGTATGGGTCAATGCTCTC	289	60	Hs
ISPD_9_F	tgtaaaacgacggccagtAATCATATGGGTTTTGAGCTTC			
ISPD_9_R	caggaaacagctatgaccGCACACACATAGATGAGTAACTTTCC	360	60	Hs
ISPD_10_F	tgtaaaacgacggccagtGCAGCAGATCTTGAAAAGTGG			
ISPD_10_R	caggaaacagctatgaccTCTACCACACACAGCAGCG	280	60	Hs
ispd_3F	GGATAATCATGACCTGATGCTG			
ispd_7R	CAGAGCCATGAACTCGTCTG	862	58	Dr
ispdi1_1F	TTCATGCGCGCGCTTAAGGAGC			
ispd_3R	GGTACCCCCGTGGACTACTTTTAC	463	58	Dr
ispdi2_1F	AATTGATAAACCCTGTCGAAATG			
ispd_3R	GGTACCCCCGTGGACTACTTTTAC	670	58	Dr
bActin_F	CCTGGGTATGGAATCTTGCG			
bActin_R	CCTGTTAGACAACTACCTCCCTTT	492	58	Dr
ispd MO1	CATGTCTGGGTTGCTCATACCCGCT			
ispd MO2	CTGCACTGCAAAGAAGAGACCAGGA	NA	NA	Dr

NA: not applicable

Supplementary Reference

1. Thisse, C. & Thisse, B. High Throughput Expression Analysis of ZF-Models Consortium Clones. (ZFIN Direct Data Submission, 2005).